A Model to Illustrate the Potential Pairing of Animal Biotelemetry with Individual-Based Modeling

Ian G Brosnan (ian.g.brosnan@nasa.gov)
NASA Ames Research Center https://orcid.org/0000-0003-2509-4325
David W Welch
Kintama Research Services, Ltd.

Research

Keywords: biotelemetry, individual-based model, acoustic tags, salmon, Columbia River

Posted Date: June 5th, 2020

DOI: https://doi.org/10.21203/rs.3.rs-29800/v1

Version of Record: A version of this preprint was published on December 11th, 2020. See the published version at https://doi.org/10.1186/s40317-020-00221-z.

Abstract

Background. Animal biotelemetry and individual-based modeling (IBM) are natural complements, but there are very few published examples where they are applied together to address fundamental or applied ecological questions. Existing studies are often found in the modeling literature and draw opportunistically on small datasets collected for purposes other than the model application. Animal biotelemetry can provide the robust measurements that capture relevant ecological patterns needed to parameterize, calibrate, and assess hypotheses in IBMs; together they could help meet demand for predictive modeling and decision-support in the face of environmental change.

Results. Using an exemplar, simple IBM that uses spatio-temporal movement patterns of 103 acoustic-tagged juvenile yearling Chinook salmon (*Oncorhynchus tshawytscha*) to quantitatively assess two migratory strategies smolts are hypothesized to use while migrating north through the plume of the Columbia River (United States of America), we find that animal biotelemetry can provide the robust measurements that capture relevant ecological patterns needed to parameterize, calibrate, and assess hypotheses in IBMs; together they could help meet demand for predictive modeling and decision-support in the face of environmental change.

Conclusions. Animal biotelemetry and individual-based modeling are now mature fields of inquiry. Our hope is that this model description and the basic analytical techniques will effectively illustrate individual-based models for the biotelemetry community, and perhaps inspire new collaborations between biotelemetry researchers and individual-based modelers.

Background

Individual-based models (IBMs) track discrete, autonomous individuals with static or dynamic state variables, attributes, and behavior, simulate interactions between them and their environment, and record the predicted effects on populations and ecosystem ecology (1) (2). As DeAngelis et al. report, they have been used in a wide variety of applied and theoretical studies within ecology, as well fields such as epidemiology, where representing individual variation was required (2) (3). IBMs are also emerging as a promising tool for predictive modeling and decision-making in the face of environmental change (4) (5) (6).

Parameterizing and calibrating individual-based models, and assessing the hypotheses they are intended to address, requires robust measurements that capture relevant ecological patterns (7). Animal biotelemetry, which focuses on the individual and has provided rich insights into survival (8), spatio-temporal movement (9), and habitat selection (10) (11) , should be a natural complement to individual-based modeling, as noted by Byron and Burke (12). However, the use of animal biotelemetry in IBMs has been limited. In just five recently published examples, two use biotelemetry data for parameterization and calibration and three extend the use of biotelemetry data to include assessing alternative hypotheses. In

nearly every case, small extant datasets were used opportunistically with limited use of quantitative methods for evaluating simulated data against observations.

Nabe-Nielsen et al. (13) and Liukkonen et al. (14) use biotelemetry data for IBM parameterization and calibration. Nabe-Nielsen et al., in a modeling framework for predicting the impacts of anthropogenic disturbances on animal movement and fitness, used statistical and visual techniques to calibrate a correlated random-walk sub-model with data from a single dead-reckoning tagged North Sea harbor porpoise (*Phocoena phocoena*), as well as dispersal parameters from 25 satellite-tagged porpoises. Biotelemetry data were not used to corroborate the model. Similarly, Liukkonen et al. used satellite telemetry data to simulate movement patterns and characterize home range formation and spatial ecology of Saimaa ringed seal (*Phoca hispida saimensis*), with the stated intent to later extend the model to study the effect of changing environmental conditions and different conservation scenarios on population dynamics. They used satellite biotelemetry data from five seals to parameterize and calibrate 'movement duration' and 'distance from home,' but used the same movement data for model validation (likely due to their small telemetry sample).

Bauduin et al. (15) and Ohashi and Sheng (16) extended the use of biotelemetry data to assessing alternative hypotheses. Bauduin et al. used VHF-based biotelemetry data from 35 Atlantic-Gaspésie caribou (*Rangifer tarandus caribou*) tracked between 1998 and 2001 to parameterize their IBM model and assess alternative movement hypotheses, including random walk, biased correlated random walk, foray loops to reproduce caribou extra-range movement patterns, and caribou fidelity during mating season. Ohashi and Sheng assess ten alternative swimming strategies, including various passive, random, and active directed movements, of juvenile Atlantic salmon (*Salmo salmar*) migrating in the Gulf of St. Lawrence. They assessed their hypotheses by comparing travel times from juveniles tagged in 2009 and 2010 against travel times of simulated salmon implemented in an ocean circulation model with numerical particle tracking. Although the original dataset included 93 tagged juvenile Atlantic salmon released into the St-Jean River, travel time was measured from only three smolts that were subsequently detected at distant sub-arrays of acoustic receivers in the Gulf of St. Lawrence.

Morrice et al. also extend the use of biotelemtry data to assess alternative hypotheses. They investigate potential migration pathways of yearling and subyearling Chinook salmon (*Oncorhynchus tshawytscha*) in the Columbia River estuary using alternative movement models; passive drift, random walk, biased correlated random walk (BCRW), and taxis for yearling Chinook and passive drift, random walk, kinesis, and area search for subyearlings. These movement models, and the migration pathways that emerged, were assessed against detections of tagged yearling and subyearling Chinook. Morrice et al.'s model is notable for the large sample of tagged animals used: 3880 yearling Chinook salmon and 4449 subyearling Chinook salmon tagged and released in 2010.

A fuller realization of the promise of IBMs and biotelemetry would include biotelemetry researchers and individual-based modelers working together at the outset of a research project. One reason why biotelemetry data is not more widely used in individual-based modeling may be limited cross-fertilization

between these fields, as evidenced by the opportunistic use of biotelemetry data in the preceding examples and publication of three of the papers in Ecological Modelling, a specialized journal whose audience may have limited overlap with the biotelemetry research community.

In an effort to bridge this gap and highlight the application of animal biotelemetry to individual-based modeling for the biotelemetry community, we present a simple IBM that uses spatio-temporal movement patterns of 103 acoustic tagged juvenile yearling Chinook salmon (smolts) to quantitatively assess two migratory strategies smolts could use while migrating north through the plume of the Columbia River (USA). These strategies include (a) maximizing growth, or (b) selectively using local currents to minimize plume occupancy time, and thus exposure to high predation pressure in the plume region. A quantitative assessment of the patterns in cross-shelf distribution of *in-silico* smolts against cross-shelf distribution from the telemetered smolts reveal that the strategy of maximizing growth is plausible, but not the selective use of coastal currents to speed passage through a predator-rich region. This model description, and the basic analytical techniques, illustrate individual-based models for the biotelemetry community and can serve as a starting point for collaborations between biotelemetry researchers and individual-based modelers.

Methods

Model Introduction

The Columbia River basin drains nearly 671,000 square kilometers of land, entering the Pacific Ocean at the border between the USA states of Oregon and Washington. The river creates a dynamic coastal river plume that juvenile yearling Chinook salmon (*Oncorhynchus tshawytscha*), 'smolts,' must navigate during the earliest stage of their marine migration (17). Previously, the plume was hypothesized to be a refuge from predators and a rich feeding ground (18), but more recent research suggests that the plume is predator-rich and with lower survival in the plume than adjacent estuarine and ocean habitats (19), (20), (21), (22), (23), (24). Due to the perceived importance of the early marine period, there has been a persistent interest in the interaction between the Columbia River plume environment and juvenile salmon migration and survival, particularly as to how migration and survival may be affected by river dynamics (25), (26), (27), (24).

Determining the effects of changing plume conditions on smolt migration and survival requires some understanding of the strategies smolts may employ during this phase of their migration. Two conceivable strategies are (a) to select habitat that maximizes growth or (b) navigate so as to minimize opposing currents during northward migration. The first strategy would be expected to reduce availability to size-selective predators while contributing to the growth necessary for them to survive their first winter at sea. This strategy is also consistent with the critical size, critical period hypothesis which posits that the adult return rate of salmon is influenced first by predation-driven mortality at ocean entry, then by starvation-driven mortality during the following winter that results from a failure to build minimum energy reserves (28).

The second strategy, navigating to minimize opposing current while migrating north, would speed northward passage, reducing the period of exposure to predation in the plume region (assuming that survival rates were lower in the plume than farther north). Brosnan et al. (29) demonstrated that survival of groups of yearling Chinook released to migrate through the plume is negatively related to their travel time, so this strategy could be beneficial. This behavior has also been observed in the field; stereovideographic studies in tributaries of the Fraser River reveal that adult sockeye salmon (*Oncorhynchus nerka*) migrating upriver selectively travel in lower current (30), and may exploit counterflowing eddies (31). Juvenile salmon are believed to similarly exploit turbulent flow during their downstream migration (32), (33).

Individual-based models are a cost-effective means of evaluating which strategy produces results consistent with observed migration patterns. The model presented here was implemented in NetLogo v.5.2, a popular Java-based software for individual-based modeling (34) and uses simulation output (salinity, temperature, and current) from the Virtual Columbia River model developed by the Center for Coastal Margin Observation and Prediction. The IBM doesn't test the effects of different strategies on plume survival, but rather which, if any, of the plausible strategies reproduces migratory patterns observed in acoustic telemetry studies of juvenile yearling Chinook—a first step in addressing the survival question.

Tagging and Telemetry

The model draws on detections of acoustic tagged juvenile yearling Chinook (*Oncorhynchus tshawytscha*) and oceanographic simulations from the 2009 spring outmigration. This dataset was chosen because tagged smolts were released from early-April through May, covering a wide range of spring ocean conditions.

VEMCO V7-2L acoustic tags were surgically implanted in 1,370 hatchery-raised Columbia River Basin juvenile yearling Chinook smolts. Acoustic receivers were deployed in subarrays across the river at Astoria Bridge and across the continental shelf at Willapa Bay to detect the passage of tagged smolts. Smolts detected on both the Astoria and Willapa Bay sub-arrays (N = 103) were used to calculate plume residence time, and the cross-shelf distribution at Willapa Bay; the relatively small sample size of 103 tracked fish is a consequence of mortality losses and the need for each included smolt to be detected on both subarrays. Greater detail on the tagging procedures and acoustic array used to track tagged smolts can be found in (29) and (35).

Individual-based Model Description

The model was implemented in NetLogo and is described here using the 'Overview, Design concepts, and Details,' or ODD, protocol of Grimm et al. (36).

Purpose

The purpose of the model was to compare two hypothesized strategies smolts may use during their northward migration through the Columbia River plume, i.e., do smolts select habitat to maximize growth, or attempt to minimize opposing currents to more quickly transit through plume region?

Entities, state variables, and scales

There were two entities in the model, ocean cells and in-silico smolts. Each ocean cell had six state variables: salinity, temperature, current velocities (x- and y-), water depth, and a representation of feeding conditions. The two types of in-silico smolts are defined by their migratory strategy, maximizing growth (MaxGro) or minimizing the current opposing their northward migration (MinCur). Each smolt, regardless of strategy, had five state variables: fork-length, weight, optimal swimming speed, heading, and a binary variable indicating whether the smolt was in estuarine (PSU < 27) or ocean (PSU $\geq$ 27) waters.

Simulations ran for 70 days in 1-hour steps. The model world origin was in the top-left grid cell, at position 3601 255000mE, 369500mN (Oregon State Plane coordinates, North American Datum of 1927) and the model extended 100 km east of the origin and 200 km south in a grid with 0.5km x 0.5 km cells. Grid cell size is the approximate distance that a 130 mm smolt (the smallest size tagged) would swim in one hour at 1 body length per second. This model world encompassed the lower Columbia River estuary and plume region, including the arrays of acoustic receivers at the Astoria Bridge and Willapa Bay.

Process overview and scheduling

A line diagram illustrating the model processes can be found in Figure 1. At each time step, eight smolts of each type were introduced into the model. To permit the last smolts introduced into the model sufficient time to migrate past Willapa Bay, the introduction of model smolts ended at time step 1250. At each step, the ocean cells updated their salinity, temperature, current velocities, and prey availability. Subsequently, each smolt calculated its weight- and temperature-dependent optimal swimming speed, evaluated whether it was in estuarine water (cell salinity < 27 PSU) or marine water (cell salinity $\geq$ 27 PSU) and moved accordingly (see below*).* Once all smolts executed their move, the model stepped forward.

Design Concepts

Pearcy (37) is widely credited with the hypothesis that the year class strength of returning salmon is established during the early marine life history, including the period of plume residency. Yearling Chinook departing the Columbia River must travel through the river plume, the dynamics of which are affected by hydropower-regulated river discharge and wind-driven currents and other oceanographic processes (38). Survival in this region is presumably affected by the migratory strategy adopted by smolts, and insight into the manner that individual smolts interact with the plume environment while migrating, revealed by patterns in their distribution across an acoustic array, could be used to evaluate the impact of changing oceanographic and river conditions (39).

In this model, smolts adapt to changes in themselves and their environment by selecting a weight and temperature-dependent swimming speed and orienting towards habitat consistent with their migratory strategy. Implementing these behaviors requires the following assumptions:

1. Smolts are assumed to employ negative rheotaxis (orientation in the direction of current) to navigate through the model estuary and into the plume. This assumption is grounded in a finding that upregulation of the hormone thyroxine in response to changing light conditions stimulates negative rheotaxis, leading smolts to travel downstream (40).
2. Smolts are assumed to have a compass sense and the ability to detect gradients in temperature, salinity, current, and prey availability. The specific mechanisms by which smolts sense these variables are not modeled, but field and laboratory observations indicate that smolts can sense gradients in the orientation and intensity of magnetic fields (41), flow (30) (42), temperature (43), and salinity (44). Their presence in trawls is also positively correlated with chlorophyll concentration and plankton abundance (45), (46), (47).
3. Smolts are assumed to begin a directed northward migration shortly after reaching the ocean, an assumption that is strongly supported by decades of U.S. and Canadian coastal trawl surveys (48), (49), (50).
4. Smolts are typically found in the top 12 m of the water column (51) and vertical migrations are assumed not to significantly affect horizontal progress, allowing the model to be collapsed into 2 spatial dimensions.

At every time step, the unique identification number, type, size, weight, local flow variables, heading, optimal swimming speed, and model coordinates (including latitude, longitude, and the corresponding grid cell) of each smolt were recorded. All model output analyses were conducted in R (52).

Initialization

The model was initialized with flow environment variables, water depth, and the simplified representation of the prey field specified from (53). Initial smolt fork lengths were assigned by drawing randomly from fork lengths of tagged smolts detected at Astoria and Willapa Bay in 2009. The fork length (FL) at tagging was adjusted for growth between release and detection at Astoria by

$$FL = FL_{tag} + 1.05 * T_{riv}$$

where FL_{tag} is the measured fork length of the tagged smolt at the time of tagging, T_{riv} is the tagged smolts travel time (d) from release to plume entry, and 1.05 (mm d^{-1}) is an observed daily growth rate in the Columbia River (49).

Input Data

The flow environment data and depth for each ocean cell at each time step was derived from DB-22, a database of Virtual Columbia River (VCR) model simulations. The VCR was built by the Center for Coastal Margin Observation and Prediction (CMOP) using SELFE, an open-source, community-supported code designed for the effective simulation of 3D baroclinic circulation in the Columbia River estuary and plume that uses semi-implicit finite-element/volume Eulerian-Lagrangian algorithms to solve the Navier-Stokes equations on unstructured triangular grids (54).

DB-22 contains flow data at 90-second intervals from the surface to the seafloor and recorded for multiple depths. To keep the computational demand tractable, flow data at 4 m, 8 m, and 12 m for each cell in the model were extracted from DB-22 in fifteen-minute intervals and then averaged and reformatted in R to create single hourly values readable by NetLogo. The choice of depth intervals is based on Emmett et al.'s (51) finding that smolts in the plume region are found in the upper 12 m of the water column.

Submodels

Submodel 1: Length-weight regression

Length-weight conversions were made using the regression model:

$$W = e^{-14.075} * FL^{3.514}$$

Where W is weight (g) and FL is fork length (mm). This is an empirical model fitted to Columbia River basin hatchery-origin yearling Chinook smolt length-weight data collected by NOAA researchers trawling at three transects in the Columbia River plume region (Columbia River, Grays Harbor, and Willapa Bay) in May and June 2008-2011 (C Morgan, NOAA, personal communication, 2013). The model was fitted to the data using the nonlinear least squares function provided in the R *stats* package (52).

Submodel 2: Optimal Swimming Speed

Optimal swimming speed was calculated using the formula described in (55) and parameterized in (56):

$$U_{opt} = ACT * W^{0.13} * e^{0.0405*T}$$

Where T is temperature and a state variable of the cell and W, weight, is a smolt state variable. ACT is a parameter from the bioenergetics submodel described below.

Submodel 3: Bioenergetics

In bioenergetics models, growth over time is estimated using a simple mass balance equation, *growth = consumption – (respiration + egestion + excretion).* This submodel uses the Wisconsin bioenergetics

equation sets (57); Table 1) for consumption (eqn. 3), respiration (eqn. 1), egestion and excretion (eqn. 2). The equations are parameterized with values from the literature on Pacific salmon bioenergetics (Table 2). Prey energy density, Q_f, is a single global parameter. All smolts use this submodel to grow. The growth-seeking model smolts use it to identify and move at a metabolically optimal speed towards habitat (grid cells) where growth opportunities are greatest.

Sensitivity analysis revealed the bioenergetics submodel to be sensitive to two parameters, prey energy density and proportion of maximum consumption, which is consistent with the findings of similar analysis reported in (55) and (58) (following (59)), as well as (60). When the bioenergetics submodel was validated by simulating migrations in the model world with bioenergetics parameters from Table 2, model smolts grew at rates consistent with a range of reported growth rates for juvenile yearling Chinook observed in the Columbia River plume region (61).

Submodel 4: Prey

A submodel representing declining prey availability with distance from shore was specified from Peterson et al.'s (53) description of three cross-shelf zones. In this sub-model, prey is represented to the model fish through the proportion of maximum consumption (bioenergetics parameter 'p_C_{max}'; (62), values of which are drawn from one of three distributions representing inshore waters (depth $\leq$ 50 m, mean 'p_C_{max}' = 0.8), mid-shelf waters (50 m < depth $\leq$ 150 m, mean 'p_C_{max}' = 0.6) and outer shelf/open water (depth > 150 m, mean 'p_C_{max}' = 0.02). Although the assignment of 'p_C_{max}' is consistent with the biomass estimates in (53) and assumptions about the volume of water searched by a transiting salmonid (63), they are a characterization, rather than a replication, of actual feeding conditions.

Submodel 5: Movement rules

In estuarine waters (PSU<27), all model smolts align with the current in their cell (negative rheotaxis). The time between exposure to marine waters and the switch to one of the two plume migration strategies occurred six hours after first exposure to marine waters (PSU$\geq$27). The timing of the switch in movement rules was calibrated using the median plume residence times of the model smolts, defined here as the median time between release and first detection on the Willapa Bay subarray. Calibration experiments indicated that a 6 h delay provided the closest match between observed plume residence times (median = 4.3 d) and plume residence time of growth maximizing smolts (median = 4.2 d) and opposing current minimizing smolts (median = 4.1 d). Model results were insensitive to variations in the switch time of ±50%.

In marine waters, smolts set their heading towards the cell north of their position with maximum growth opportunity or minimum southward flowing current that it could reach in one hour at its optimal swimming speed. Smolts moved to the terminal point of a vector that was addition of their movement vector (heading, optimal speed) and the current vector in the cell they occupied. If the smolt's final position was outside the north, south, or west bounds of the model, the smolt was considered to have

permanently emigrated, otherwise it grew according to the bioenergetics submodel. In the estuary, smolts were not permitted to swim east (upriver) of the model boundary.

Submodel 6: Simulated detections

Detections of model smolts on the Willapa Bay subarray receivers were simulated by evaluating smolt paths (Euclidean lines drawn between smolt positions at each model step) to determine if they overlapped any of the detection zones centered on each receiver. The estimated detection range of the acoustic tags was 400 meters. For each smolt path that intersected a receiver's detection radius, the receiver number, smolt number, and time of detection were recorded. Model detections on virtual receivers corresponding to those that were lost during the 2011 season were recorded, but removed prior to analyzing the cross-shelf distributions against observed values.

Model Output Analysis

Model output analyses, including simulated detections, were conducted in R. The cross-array distribution of detections of tagged smolts and model smolts was compared using a modified Cramer von-Mises test (64), where the null hypothesis is that there is no difference in the distributions. Syrjala's (64) test was calculated using the R package *ecespa*, and summary circular statistics using *circular*.

Model Results

At a significance level of 0.05, there was no difference in the distributions of the MaxGro smolts and tagged smolts (*p-value* = 0.54; Figure 2). There was a significant difference in the distributions of the MinCur smolts and tagged smolts (*p-value* = 0.02; Figure 2). Model smolt tracks (Figure 3) reveals a more bifurcated pattern in the MinCur types tracks; they traveled close inshore when wind-driven transport was easterly (downwelling), and offshore when westerly (upwelling). MaxGro tracks showed a similar pattern, but their sensitivity to modeled feeding conditions resulted in their being retained on the shelf, and more evenly distributed. The number of smolts crossing the virtual subarray at Willapa Bay was sensitive to the magnitude and direction of wind-driven coastal transport.

Discussion Of The Individual-based Model

The results from the individual-based model suggest that smolts may pursue a strategy of maximizing growth upon beginning their northward migration. Under the critical size, critical period hypothesis, which posits that adult returns are affected first by predation at marine entry, and then starvation during the first winter, this strategy could improve the probability of survival if smolts grow to exceed the gape size of predators and attain sufficient energy reserves to avoid winter starvation. Additionally, the model indicates that strong westward transport advects smolts off the shelf; a prediction that cannot currently be validated, but could affect survival. Pearcy (37) noted that alongshore or offshore displacement of juveniles immediately after ocean entry could reduce predation and enhance survival. Findings by Brosnan et al. (29) that travel time affects plume survival supports this notion.

However, while it might seem that the selective use of alongshore current by model smolts employing the MinCur strategy would speed passage out of the plume region and enhance survival, this behavior proved to reduce travel time to Willapa Bay by only a few hours relative to the MaxGro strategy. Applying the survival equation used in (29) to estimate survival to the Willapa Bay subarray using median travel times suggests that survival would be virtually indistinguishable between the growth maximizing smolts and current minimizing smolts (0.60 v 0.61, respectively) that reach the array. This suggests there may be little benefit to the active use of favorable current gradients in the plume region.

In addition to the apparently limited survival benefit of selective use of coastal currents in the plume region, there are additional reasons why this pattern may not extend beyond the river. First, the high density of salmon in the river raises the costs of competing for limited food resources and salmon may restrict their feeding and perform the river migration on a limited energy budget (65), (40); but see (66) for evidence that smolt feeding increases in the lower Columbia River. Thus, there may be strong pressure to minimize the cost of migration in the river. Conversely, the early marine environment represents a rich feeding ground where a delay in feeding could result in smolts failing to meet the energy requirements to survive their first winter at sea (28).

Second, the confined river environment provides turbulent flow and relative motion cues from the riverbed and similar features that salmon demonstrably respond to (30), (42). Beyond the tidal plume, these cues are weakened. During the spring, flow in the lower Columbia River is approximately 1 m s^{-1} (and can be much greater) and exceeds 3 m s^{-1} in the tidal outflow at the river mouth, whereas ambient coastal current velocity is approximately 0.1 m s^{-1} (67), (25). Shear turbulence is likely reduced in the coastal ocean, and smolts are not positioned to use the seabed as a frame of reference (51). Conceivably, they can detect the fine-scale changes in the intensity of turbulence and/or their motion relative to celestial objects and the earth's magnetic field. This would allow them to take advantage of small, favorable gradients in coastal current. However, they would require very sensitive absolute and differential thresholds to these cues, which have not been determined experimentally.

The successful transition from river to ocean requires that smolts complete a number of changes (i.e., smoltification). The precise trigger, or series of triggers, during this complex process that result in the behavioral transition to directed northward migration in the ocean have not been determined. It may be driven by hormonal changes prompted by environmental cues, much as up regulation of thyroxine triggers downstream migration (40). We attempted to capture the transition via a simple threshold-delayed response model, but a mechanistic understanding of the process might explain why smolts are occasionally detected migrating at least as far south as Cascade Head, OR, before turning and swimming north (68).

Incorporating a representation of coastal feeding conditions acted to contain the MaxGro smolts on the shelf, but the fact that nearly 20% of the MaxGro smolts still migrated outside the bounds of the subarray at Willapa Bay is a potentially interesting result. Burke et al. (69) report similar results, although they interpret it as a modeling problem and describe using an Ornstein-Uhlenbeck process that forced model

fish to orient towards the historic centers of mass of juvenile salmon sampled across the shelf in an attempt to correct it. Trawl surveys and acoustic receiver subarrays terminate near the shelf break because few or no fish are caught in trawls near the shelf break. Results from this model suggest that there could be a bi-modal distribution of catches/detections that would not be detected under the current sampling regime.

As Pearcy (37) notes, this could have implications for early marine survival. Columbia River basin smolts driven off-shelf at ocean entry might experience reduced predation pressure, particularly from seabirds nesting near the river mouth (19), (24). Their feeding opportunities would likely be reduced (45), (53), but directed northward migration would lead them to quickly regain the shelf environment, which arcs westward north of the Columbia River. Outmigrating yearling Chinook would be placed to take advantage of this offshore transport and potentially reduce their risk of predation since the necessary conditions occur in early spring, when the transition to the upwelling season is beginning and winds are strong.

A second outcome of the model was that negative rheotaxis was sufficient to guide smolts out of the estuary. The initial expectation was that the tidally-reversing flow of the Columbia River would significantly delay, or prevent, progress towards the ocean, whereas McInerney (70) reasoned that preference for increasing salinity could serve as an orientation mechanism for smolts in the estuary. However, whether salmon use salinity to orient remains unresolved (12) and the two mechanisms were compared during model development. Both produced similar migratory patterns, although orientation by negative rheotaxis resulted in smolts initially traveling further offshore under west transport conditions than did orientation by salinity. Negative rheotaxis was selected for the final model because it has a known biochemical basis wherein increasing day length stimulates the upregulation of thyroxine, which in turn causes smolts to orient with the current (40).

Railsback et al. (71) proposed a condition-based movement rule for stream fish in IBM's, termed *expected survival*, where fish move to habitat where the probability of surviving non-starvation mortality risks, multiplied by the probability of surviving starvation risk over a pre-determined time horizon, is greatest. Yearling Chinook in the marine environment appear to respond to feeding conditions during northward migration, so applying Railsback et al.'s (71) *expected survival*, using the first-winter critical period as the time horizon, may be a fruitful development of the IBM presented here. This would require collaboration among researchers who have collected data on salmon predators, salmon prey, and early marine survival to develop a more accurate representation of predator and prey fields than are currently captured by the IBM; such data are now becoming available (e.g., (24)).

Conclusion

The foregoing model is intended to illustrate the pairing of animal biotelemetry data and individual-based models by highlighting simple ways that biotelemetry data can be used for better informing the development of an IBM. Conditions appear ripe for a productive pairing of individual-based modeling and animal biotelemetry. First, although the body of literature describing IBMs implemented with biotelemetry

data is limited and relies largely on repurposing of existing small datasets (but see (11) for re-use of a much larger biotelemetry dataset), it is a promising sign of active interest among individual-based modelers in using biotelemetry data. Second, national and international data assembly, archiving, and access efforts such as the U.S. Animal Tracking Network (atn.ioos.us), the Ocean Tracking Network (oceantrackingnetwork.org), and the International Movebank animal tracking database (www.movebank.org) will make more data discoverable and accessible. This will create opportunities to aggregate datasets sufficient for robust IBM parameterization, calibration, and hypothesis testing. Still, the fact that animal biotelemetry data is expensive to collect and requires experience and specialized skills for most elements of array design and deployment, tagging, and data processing and analysis will still require partnerships for prospective projects. Finally, as individual-based modeling and animal biotelemetry have matured, many of the challenges of implementing a successful biotelemetry-supported IBM activity have been identified and overcome. Researchers have access to a wealth of methodological information in specialized journals and textbooks (1) (72) and a multitude of proven software tools for modeling and analysis.

Abbreviations

BCRW: biased correlated random walk

CMOP: Center for Coastal Margin Observation and Prediction

IBM: Individual-based Model

MaxGro: a type of model smolt that employs a maximizing growth strategy

MinCur: a type of model smolt that employs a strategy of minimizing currents that oppose their northward migration

VCR: Virtual Columbia River (VCR) model simulations.

Declarations

Ethics approval and consent to participate: Not applicable.

Consent for publication: Not applicable.

Availability of data and materials: Acoustic telemetry data used in this study are available from Kintama Research Services upon request. Virtual Columbia River simulation outputs used in this study are available from IGB upon request and with permission of the Center for Coastal Margin Observation and Prediction.

Competing interests: The authors declare that they have no competing interests.

Funding: IGB gratefully acknowledges the support of the U.S. Department of Defense, through the National Defense Science and Engineering Graduate Fellowship Program, and the Atkinson Center for a Sustainable Future. The U.S. Department of Energy, Bonneville Power Administration, provided funding to Kintama (Contract No. 52071, Project Number 2003-114-00). The funding bodies had no role in the design of the study, collection, analysis, interpretation of data, nor writing the manuscript.

Authors' contributions: IGB conceived and executed the individual-based modeling effort and wrote the draft manuscript. DWW conceived/supervised the salmon acoustic telemetry project, and provided advice in developing the individual-based model and reviewing/editing the manuscript. Both authors read and approved the final manuscript.

Acknowledgements: This work would not have been possible without the support of the Kintama team, including Aswea Porter, Erin Rechisky, Paul Winchell, Melinda Jacobs Scott, as well as Antonio Baptista, Paul Turner, and the team at the Center for Coastal Margin Observation and Prediction, who opened their databases and facilitated access.

References

1. Railsback SF, Grimm V. Agent-Based and Individual-Based Modeling: A Practical Introduction Princeton: Princeton University Press; 2012.

2. DeAngelis DL, Grimm V. Individual-based models in ecology after four decades. F1000Prime Reports. 2014 June; 6(39): p. 6-39.

3. DeAngelis DL, Mooij WM. Individual-Based Modeling of Ecological and Evolutionary Processes. Annual Review of Ecology, Evolution, and Systematics. 2005 December; 36: p. 147-168.

4. Stillman RA, Railsback SF, Giske J, Berger U, Grimm V. Making Predictions in a Changing World: The Benefits of Individual-Based Ecology. Bioscience. 2015 February; 65(2): p. 140-150.

5. Wood KA, Stillman RA, Goss-Custard JD. Co-creation of individual-based models by practitioners and modellers to inform environmental decision-making. Journal of Applied Ecology. 2015 August; 52(4): p. 810-815.

6. Beltran RS, Testa JW, Burns JM. An agent-based bioenergetics model for predicting impacts of environmental change on a top marine predator, the Weddell seal. Ecological Modelling. 2017 May; 351: p. 36-50.

7. Volker G, Railsback SF. Patttern-oriented modelling: a 'multi-scope' for predictive systems ecology. Philosophical transactions of the Royal Society of London. Series B, Biological Sciences. 2012; 367(1588): p. 293-310.

8. Rechisky EL, Porter AD, Clark TD, Furey NB, Gale MK, Hinch SG, et al. Quantifying survival of age-2 Chilko Lake sockeye salmon during the first 50 days of migration. Canadian Journal of Fisheries and Aquatic Sciences. 2018.

9. Taylor MD, Laffan SW, Fairfax AV, Payne NL. Finding their way in the world: Using acoustic telemetry to evaluate relative movement patterns of hatchery-reared fish in the period following release. Fisheries Research. 2017 February; 186(2): p. 538-543.

10. Lea SE, Humphries NE, von Brandis RG, Clarke CR, Sims DW. Acoustic telemetry and network analysis reveal the space use of multiple reef predators and enhance marine protected area design. Proceedings of the Royal Society B. 2016 July; 283(1834).

11. Morrice KJ, Baptista AM, Burke BJ. Environmental and behavioral controls on juvenile Chinook salmon migration pathways in the Columbia River estuary. Ecological Modelling. 2020 July 1; 427(109003).

12. Byron CJ, Burke BJ. Salmon ocean migration models suggeest a variety of population-specific strategies. Reviews in Fish Biology and Fisheries. 2014 September; 24: p. 737-756.

13. Nabe-Nielsen J, van Beest FM, Grimm V, Sibly RM, Teilmann J, Thompson PM. Predicting the impacts of anthropogenic disturbances on marine populations. Conservation Letters. 2018 May; 11(5): p. e12563.

14. Liukkonen L, Ayllon D, Kunnasranta M, Niemi M, Nabe-Nielsen J, Grimm V, et al. Modelling movements of Saimaa ringed seals using an individual-based approach. Ecological Modelling. 2018 January; 368: p. 321-335.

15. Bauduin S, McIntire E, St-Laurent MH, Cumming S. Overcoming challenges of sparse telemetry data to estimate caribou movement. Ecological Modelling. 2016 September 10; 335: p. 24-34.

16. Ohashi K, Sheng J. Study of Atlantic salmon post-smolt movement in the Gulf of St. Lawrence using an individual-based model. Regional Studies in Marine Science. 2018; 2018: p. 113-132.

17. U.S. Geological Survey. River Basins of the United States: The Columbia. Report. U.S. Geological Survey, Department of the Interior; 1981. Report No.: 10.3133/70039373.

18. Casillas E. Role of the Columbia River estuary and plume in salmon productivity. In Bisbal GA, editor. Proceedings of the Symposium on Ocean Conditions and the Management of Columbia River Salmon; 1999; Portland: Northwest Power Planning Council. p. 55-84.

19. Collis K, Roby DD, Craig DP, Adamany S, Adkins JY, Lyons DE. Colony Size and Diet Composition of Piscivorous Waterbirds on the Lower Columbia River: Implications for Losses of Juvenile Salmonids to Avian Predation. Transactions of the American Fisheries Society. 2002; 131(3): p. 537-550.

20. Anderson CD, Roby DD, Collis K. Foraging patterns of male and female Double-breasted Cormorants nesting in the Columbia River estuary. Canadian Journal of Zoology. 2004; 82(4): p. 541-554.

21. Lyons DE, Roby DD, Collis K. Foraging Ecology of Caspian Terns in the Columbia River Estuary, USA. Waterbirds: The International Journal of Waterbird Biology. 2005; 28(3): p. 280-291.

22. Emmett RL, Krutzikowsky GK, Bentley P. Abundance and distribution of pelagic piscivorous fishes in the Columbia River plume during spring/early summer 1998–2003: Relationship to oceanographic conditions, forage fishes, and juvenile salmonids. Progress in Oceanography. 2006 January; 68(1): p. 1-26.

23. Porter AD, Welch DW, Rechisky EL, Jacobs Scott MC. Marine and freshwater mortality of delayed and differential-delayed mortality of Columbia & Snake River yearling Chinook smolts using a continental-scale acoustic telemetry array, 2011. Report to Bonneville Power Administration. Kintama Research Services; 2011. Report No.: Contract No. 52071, Project No. 2003-114-00.

24. Phillips EM, Horne JK, Zamon JE. Predator–prey interactions influenced by a dynamic river plume. Canadian Journal of Fisheries and Aquatic Sciences. 2017; 74(9): p. 1375-1390.

25. Jay DA, Pan J, Orton PM, Horner-Devine AR. Asymmetry of Columbia River tidal plume fronts. Journal of Marine Systems. 2009 October; 78(3): p. 442-459.

26. Burla M, Baptista AM, Casillas E, Williams JG, Marsh DM. The influence of the Columbia River plume on the survival of steelhead (Oncorhynchus mykiss) and Chinook salmon (Oncorhynchus tshawytscha): a numerical exploration. Canadian Journal of Fisheries and Aquatic Sciences. 2010; 67(10): p. 1671-1684.

27. Miller JA, Teel DJ, Baptista A, Morgan CA. Disentangling bottom-up and top-down effects on survival during early ocean residence in a population of Chinook salmon (Oncorhynchus tshawytscha). Canadian Journal of Fisheries and Aquatic Science. 2013; 70(4): p. 617-629.

28. Beamish RJ, Mahnken C. A critical size and period hypothesis to explain natural regulation of salmon abundance and the linkage to climate and climate change. Progress in Oceanography. 2001; 49(1-4): p. 423-437.

29. Brosnan IG, Welch DW, Erin RL, Porter AD. Evaluating the influence of environmental factors on yearling Chinook salmon survival in the Columbia River plume (USA). Marine Ecology Progress Series. 2014; 496: p. 181-196.

30. Standen E, Hinch SG, Rand PS. Influence of river speed on path selection by migrating adult sockeye salmon (Oncorhynchus nerka). Canadian Journal of Fisheries and Aquatic Sciences. 2004; 61(6): p. 905-912.

31. Hinch SG, Rand PS. Optimal swimming speeds and forward-assisted propulsion: energy-conserving behaviours of upriver-migrating adult salmon. Canadian Journal of Fisheries and Aquatic Sciences. 2000; 57(12): p. 2470-2478.

32. Coutant C, Whitney R. Fish Behavior in Relation to Passage through Hydropower Turbines: A Review. Transactions of the American Fisheries Society. 2000; 129(2): p. 351-380.

33. Tiffan KF, Kock TJ, Haskell CA, Connor WP, Steinhorst RK. Water Velocity, Turbulence, and Migration Rate of Subyearling Fall Chinook Salmon in the Free-Flowing and Impounded Snake River. Transactions of the American Fisheries Society. 2009; 138(2): p. 373-384.

34. Wilensky U. NetLogo. http://ccl.northwestern.edu/netlogo.

35. Porter AD, Welch DW, Rechisky EL, Jacobs-Scott MC, Lydersen H, Winchell PM, et al. Marine and Freshwater Measurement of Delayed and Differential-Delayed Mortality of Snake River Spring Chinook Smolts Using a Continental-Scale Acoustic Telemetry Array, 2009. Report to Bonnevilee Power Administration, Contract No. 46389, Project No. 2003-114-00. Kintama Research Services; 2010.

36. Grimm V, Berger U, DeAngelis DL, Polhill JG, Giske J, Railsback F. The ODD protocol: A review and first update. Ecological Modelling. 2010 November; 221(23): p. 2760-2768.

37. Pearcy WG. Ocean Ecology of North Pacific salmonids Seattle: Washington Sea Grant Program; 1992.

38. Burla M, Baptista AM, Zhang Y, Frolov S. Seasonal and interannual variability of the Columbia River plume: A perspective enabled by multiyear simulation databases. Journal of Geophysical Research. 2010; 115(C2): p. C00B16.

39. Wood KA, Stillman RA, Goss-Custard JD. Co-creation of individual-based models by practitioners and modellers to inform environmental decision-making. Journal of Applied Ecology. 2015; 52(4): p. 810-815.

40. Cooke SJ, Crossin GT, Hinch SG. Pacific Salmon Migration: Completing the Cycle. In Farrell AP, Stevens ED, Cech JJ, Richards JG, editors. Encyclopedia of Fish Physiology: From Genome to Environment. San Diego: Academic Press; 2011. p. 1945-1952.

41. Putnam NF, Scanlan MM, Billman EJ, O'Neil JP, Couture RB, Quinn TP, et al. An Inherited Magnetic Map Guides Ocean Navigation in Juvenile Pacific Salmon. Current Biology. 2014 February 17; 24(4): p. 446-450.

42. Kemp PS, Williams JG. Response of migrating Chinook salmon (Oncorhynchus tshawytscha. River Research and Applications. 2008; 24: p. 571-579.

43. Hinke JT, Foley DG, Wilson C, Watters GM. Persistent habitat use by Chinook salmon (Oncorhynchus tshawytscha) in the coastal ocean. Marine Ecology Progress Series. 2005; 304: p. 207-220.

44. Healey MC. Utilization of the Nanaimo River estuary British Columbia Canada by juvenile Chinook salmon, Oncorhynchus tshawytscha. Fishery Bulletin. 1980; 77(3): p. 653-668.

45. Bi H, Ruppel RE, Peterson WT. Modeling the pelagic habitat of salmon off the Pacific Northwest (USA) coast using logistic regression. Marine Ecology Progress Series. 2007; 336: p. 249-265.

46. Bi H, Peterson WT, Lamb J, Caillas E. Copepods and salmon: characterizing the spatial distribution of juvenile salmon along the Washington and Oregon coast, USA. Fisheries Oceanography. 2011; 20(2): p. 125-138.

47. Yu H, Bi H, Burke BJ, Peterson WT. Spatial variations in the distribution of yearling spring Chinook salmon off Washington and Oregon using COZIGAM analysis. Marine Ecology Progress Series. 2012; 465: p. 253-265.

48. Miller DR, Williams JG, Sims CW. Distribution, abundance, and growth of juvenil salmonids off

the coast of Oregon and Washington, Summer 1980. Fisheries Research. 1983; 2(1): p. 1-17.

49. Fisher JP, Pearcy WG. Distribution, migration, and growth of juvenile Chinook salmon, Oncorhynchus tshawytscha. Fishery Bulletin. 1995; 93: p. 274-289.

50. Trudel M, Fisher J, Orsi JA, Morris JF, Thiess ME, Sweeting RM, et al. Distribution and Migration of Juvenile Chinook Salmon Derived from Coded Wire Tag Recoveries along the Continental Shelf of Western North America. Transactions of the American Fisheries Society. 2009; 138(6): p. 1369-1391.

51. Emmett RL, Brodeur RD, Orton PM. The vertical distribution of juvenile salmon (Oncorhynchus spp.) and associated fishes in the Columbia River plume. Fisheries Oceanography. 2004; 13(6): p. 392-402.

52. Team RDC. R: a language and environment for statistical computing. 2011. Available at: www.rproject.org.

53. Peterson WT, Morgan CA, Fisher JP, Casillas E. Ocean distribution and habitat associations of yearling coho (Oncorhynchus kisutch) and Chinook (O. tshawytscha) salmon in the northern California Current. Fisheries Oceanography. 2010; 19(6): p. 508-525.

54. Zhang Y, Baptista M. SELFE: A semi-implicit Eulerian–Lagrangian finite-element model for cross-scale ocean circulation. Ocean Modelling. 2008; 21(3-4): p. 71-96.

55. Stewart DJ, Weininger D, Rottiers DV, Edsall TA. An Energetics Model for Lake Trout, Salvelinus namaycush: Application to the Lake Michigan Population. Canadian Journal of Fisheries and Aquatic Sciences. 1983; 40(6): p. 681-698.

56. Stewart DJ, Ibarra M. Predation and Production by Salmonine Fishes in Lake Michigan, 1978–88. Canadian Journal of Fisheries and Aquatic Sciences. 1991; 48(5): p. 909-922.

57. Hanson PC, Johnson TB, Schindler DE, Kitchell JF. Fish Bioenergetics 3.0. Technical Report. ; 1997. Report No.: WISC-T-97-001.

58. Beauchamp DA, Cross AD, Armstrong JL, Myers KW, Moss JH, Boldt JL, et al. Bioenergetic Responses by Pacific Salmon to Climate and Ecosystem Variation. North Pacific Anadromous Fish Commission Bulletin 4. 2007;: p. 257-269.

59. Kitchell JF, Stewart DJ, Weininger D. Applications of a Bioenergetics Model to Yellow Perch (Perca flavescens) and Walleye (Stizostedion vitreum vitreum). Journal of the Fisheries Research Board of Canada. 1977; 34(10): p. 1922-1935.

60. Railsback F, Rose KA. Bioenergetics Modeling of Stream Trout Growth: Temperature and Food Consumption Effects. Transactions of the American Fisheries Society. 1999; 128: p. 241-256.

61. Tomaro LM, Teel DJ, Peterson WT, Miller JA. When is bigger better? Early marine residence of middle and upper Columbia River spring Chinook salmon. Marine Ecology Progress Series. 2012; 452: p. 237-252.

62. Brodeur RD, Francis RC, Pearcy WG. Food consumption of juvenile coho (Oncorhynchus kisutch) and Chinook salmon (O. tshawytscha) on the continental shelf off Washington and Oregon. Canadian Journal of Fisheries and Aquatic Sciences. 1992; 49(8): p. 1670-1685.

63. Mazur MM, Beauchamp DA. A comparison of Visual Prey Detection Among Species of Piscivorous Salmonids: Effects of Light and Low Turbidities. Environmental Biology of Fishes. 2003; 67(4): p. 397-405.

64. Syrjala SE. A Statistical Test for a Difference between the Spatial Distributions of Two Populations. Ecology. 1996 January; 77(1): p. 75-80.

65. Quinn TP. The behavior and ecology of Pacific Salmon and Trout Seattle: University of Washington Press; 2005.

66. Muir WD, Coley C. Diet of Yearling Chinook Salmon and Feeding Success During Downstream Migration in the Snake and Columbia Rivers. Northwest Science. 1996; 70(4): p. 298-305.

67. Hickey BM. Patterns and processes of shelf and slope circulation. In Landry MR, Hickey BM, editors. Coastal Oceanography of Washington and Oregon. Amsterdam: Elsevier; 1989. p. 41-115.

68. Rechisky EL, Welch DW, Porter AD, Hess JE, Narum SR. Testing for delayed mortality effects in the early marine life history of Columbia River Basin yearling Chinook salmon. Marine Ecology Progress Series. 2014; 496: p. 159-180.

69. Burke BJ, Anderson JJ, Baptista AM. Evidence for multiple navigational sensory capabilities by Chinook salmon. Aquatic Biology. 2014; 20: p. 77-90.

70. McInerney JE. Salinity Preference: an Orientation Mechanism in Salmon Migration. Journal of the Fisheries Research Board of Canada. 1964; 21(5): p. 995-1018.

71. Railsback SF, Lamberson RH, Harvey BC, Duffy WE. Movement rules for individual-based models of stream fish. Ecological Modelling. 1999; 123: p. 73-89.

72. Klimley AP. Why publish Animal Biotelemetry. Animal Biotelemetry. 2013 February 26; 1(1): p. 1-3.

73. Railsback SF, Grimm V. Agent-Based and Individual-Based Modeling Princeton: Princeton University Press; 2012.

Tables

Table 1. Bioenergetics equations

Consumption	$C = C_{max} * p\_C_{max} * f(T)$ $C_{max} = CA * W^{CB}$ $f(T) = K_A * K_B$ $K_A = \frac{CK1 * L1}{1 + CK1 * (L1 - 1)}$ $L1 = e^{G1 * (T - CQ)}$ $G1 = \frac{1}{CTO - CQ} * \ln\frac{0.98 * (1 - CK1)}{CK1 * 0.02}$ $K_B = \frac{CK4 * L2}{1 + CK4 * (L2 - 1)}$ $L2 = e^{G2 * (CTL - T)}$ $G2 = \frac{1}{CTL - CTM} * \ln\frac{0.98 * (1 - CK4)}{CK4 * 0.02}$
Respiration	$R = RA * W^{RB} * f(T) * ACTIVITY$ $S = SDA * (C - F)$ $f(T) = e^{RQ * T}$ $ACTIVITY = e^{RTO * VEL}$ if $T > RTL$, $VEL = RK1 * W^{RK4}$ if $T \leq RTL$, $VEL = ACT * W^{RK4} * e^{BACT * T}$
Egestion	$F = FA * T^{FB} * e^{FG * p\_CC_{max}} * C$
Excretion	$U = UA * T^{UB} * e^{UG * p\_CC_{max}} * (C - F)$

Table 2. Bioenergetics sub-model parameters

	Parameter Description	Symbol	Value	Source
Consumption	Intercept: C_{max}	CA	0.303 (g g^{-1} d^{-1})	Stewart & Ibarra 1991
	Coefficient: C_{max} *vs. weight*	CB	-0.275	Stewart & Ibarra 1991
	Proportion of C_{max}	p_C_{max}	0.6	Brodeur et al. 1992
	Temperature for K_1	CQ	5 (°C)	Stewart & Ibarra 1991
	Temperature for K_2	CTO	15 (°C)	Stewart & Ibarra 1991
	Temperature for K_3	CTM	18 (°C)	Stewart & Ibarra 1991
	Temperature for K_4	CTL	24 (°C)	Stewart & Ibarra 1991
	Proportion C_{max} at θ_1	CK1	0.36	Stewart & Ibarra 1991
	Proportion C_{max} at θ_4	CK4	0.01	Stewart & Ibarra 1991
Respiration	Intercept: *R*	RA	0.00264 (g 0_2 d^{-1})	Stewart & Ibarra 1991
	Coefficient: *R vs. weight*	RB	-0.217	Stewart & Ibarra 1991
	Coefficient: *R vs. temperature*	RQ	0.06818	Stewart & Ibarra 1991
	Coefficient: *R vs. swim speed U*	RTO	0.0234	Stewart & Ibarra 1991
	Intercept: *U*	ACT	9.7 (cm s^{-1})	Stewart & Ibarra 1991
	Coefficient: *U vs. weight*	RK4	0.13	Stewart & Ibarra 1991
	Intercept: *swim speed over cutoff temperature*	RK1	1 (cm s^{-1})	Stewart & Ibarra 1991
	Cutoff temperature for activity relationship	RTL	25 (°C)	Stewart & Ibarra 1991
	Coefficient: *U vs. temperature*	BACT	0.0405	Stewart & Ibarra 1991
	Specific dynamic action	SDA	0.172	Stewart & Ibarra 1991
Egestion	Intercept: *proportion egested vs. temperature and ration*	FA	0.212	Stewart & Ibarra 1991
	Coefficient: *temperature vs. egestion*	FB	-0.222	Stewart & Ibarra 1991
	Coefficient: *p versus egestion*	FG	0.631	Stewart & Ibarra 1991
Excretion	Intercept: *proportion excreted vs. temperature and ration*	UA	0.0314	Stewart & Ibarra 1991
	Coefficient: *temperature vs. excretion*	UB	0.58	Stewart & Ibarra 1991
	Coefficient: *p versus excretion*	UG	-0.299	Stewart & Ibarra 1991
Energy Density	Intercept: *(kJ/g) versus predator body weight (W)*	a	4.18	Trudel et al. 2005
	Coefficient: *(kJ/g) versus predator body weight (W)*	b	0.0025	Trudel et al. 2005
	Conversion *(kJ to J)*	c	1000	[*Wisconsin equations require J/g*]
	Energy density of prey	Qf	4200	Trudel et al. 2005, citing Davis et al. 1998

Figures

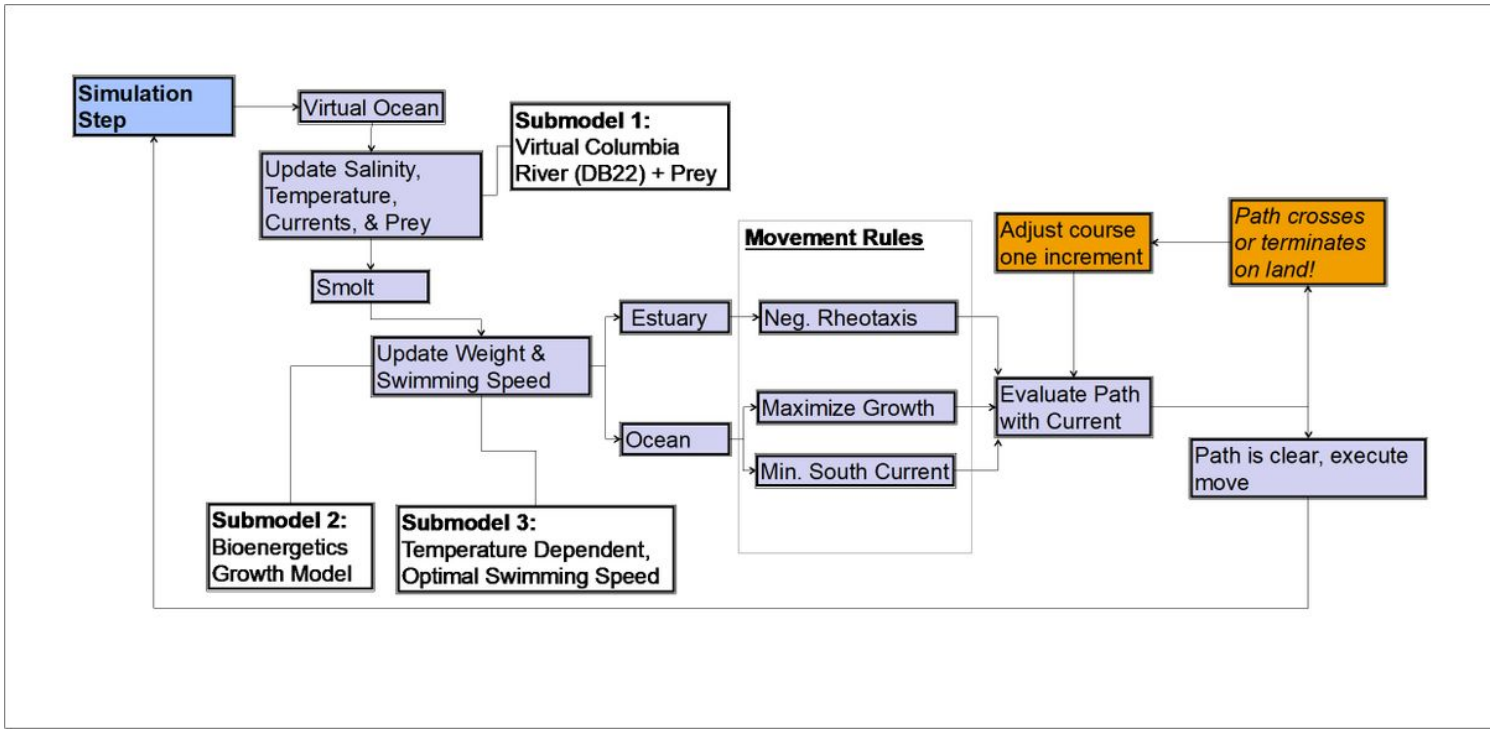

Figure 1

Process Overview Diagram. The origin is at the top left blue box entitled “Simulation Step”. Purple boxes delineate the process, orange boxes delineate the algorithm for ensuring smolts do not cross or move to land, and white boxes indicate sub-model routines.

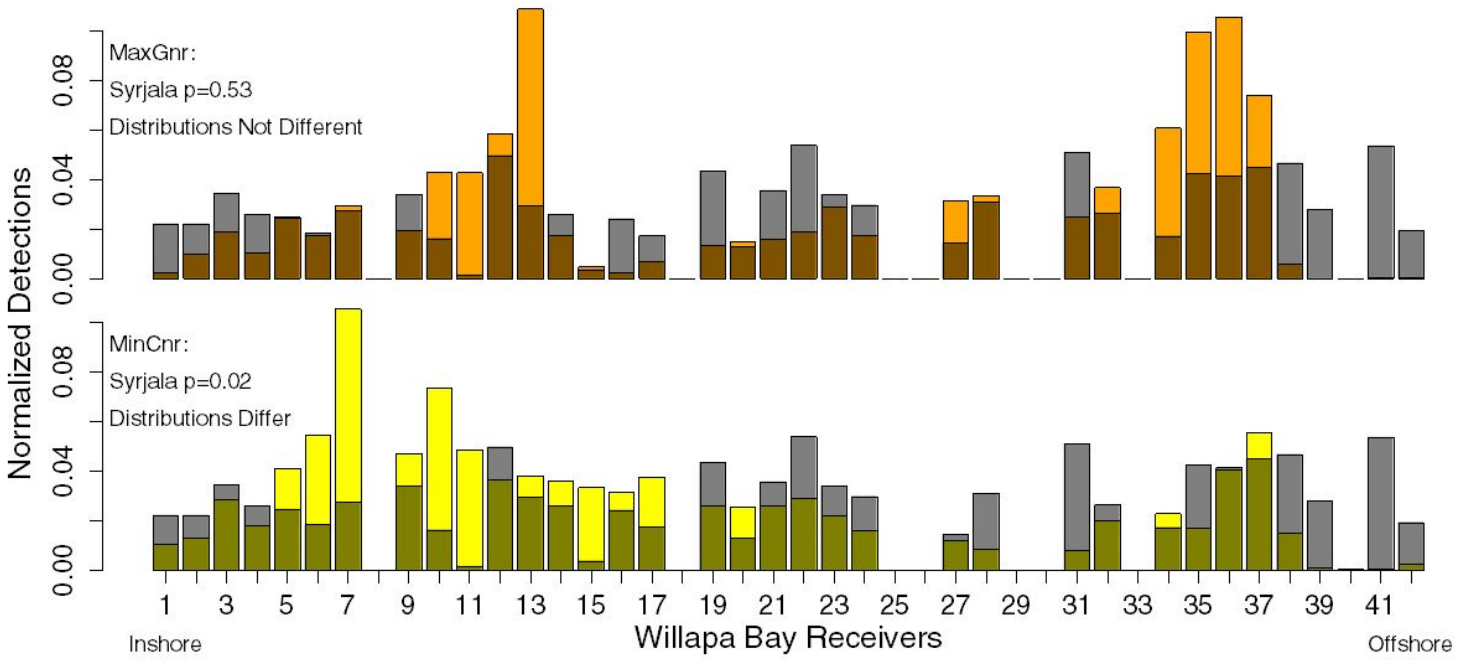

Figure 2

Cross-shelf distribution of detections on the Willapa Bay sub-array of receivers of MaxGro (top panel, orange bars) and MinCur (bottom panel, yellow bars) smolts overlaid on detections of live, tagged smolts (both panels, gray bars). Results in the top left corner of each panel are from a modified Cramer von-Mises (Syrjala 2006) test for different distributions. The MinCnr smolts appear to have a more inshore distribution across the array than observed or MaxGnr smolts, likely reflecting their use of a coast-hugging, north-flowing plume that develops with westerly winds.

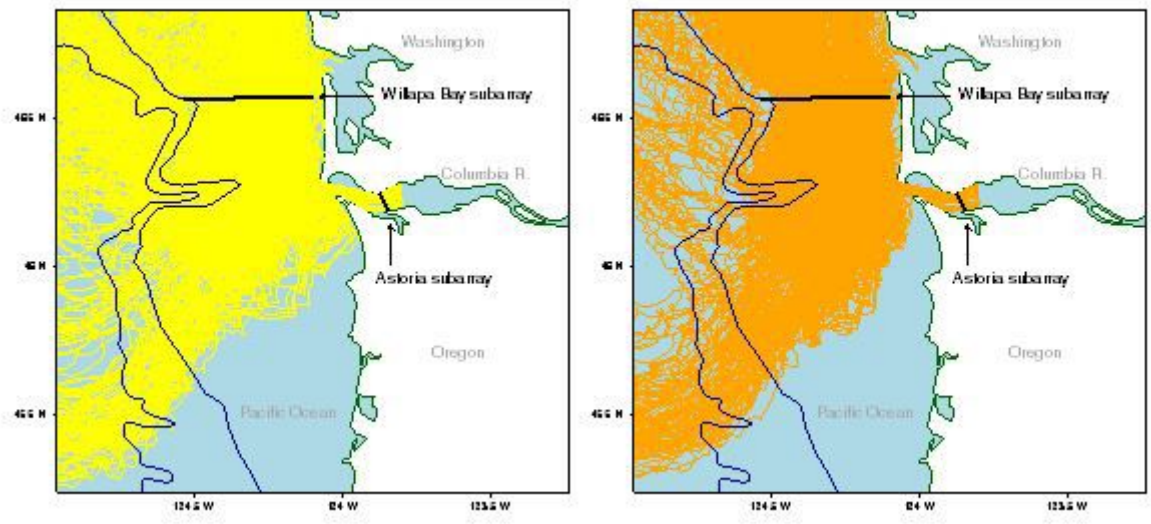

Figure 3

In-silico MinCur (L) and MaxGro (R) smolt tracks. To reduce clutter, only the track of the first smolt released at each step is displayed. Contour lines mark the 200 m and 500 m isobaths.